journal of the mechanical behavior of biomedical materials 113 (2021) 104113

Contents lists available at ScienceDirect

Journal of the Mechanical Behavior of Biomedical Materials

journal homepage: http://www.elsevier.com/locate/jmbbm

Transient stiffening of cartilage during joint articulation: A microindentation study

Catherine Yuh [a,*], Michel P. Laurent [a], Rosa M. Espinosa-Marzal [b], Susan Chubinskaya [a], Markus A. Wimmer [a]

[a] Rush University Medical Center, Chicago, IL, USA
[b] University of Illinois at Urbana-Champaign, Urbana, IL, USA

ARTICLE INFO

Keywords:
Cartilage
Articular loading
Tribology
Microindentation
Superficial zone

ABSTRACT

As a mechanoactive tissue, articular cartilage undergoes compression and shear on a daily basis. With the advent of high resolution and sensitive mechanical testing methods, such as micro- and nanoindentation, it has become possible to assess changes in small-scale mechanical properties due to compression and shear of the tissue. However, investigations on the changes of these properties before and after joint articulation have been limited. To simulate articular loading of cartilage in the context of human gait, a previously developed bioreactor system was used. Immediately after bioreactor testing, the stiffness was measured using microindentation. Specifically, we investigated whether the mechanical response of the tissue was transient or permanent, dependent on counterface material, and an effect limited to the superficial zone of cartilage. We found that cartilage surface stiffness increases immediately after articular loading and returns to baseline values within 3 hr. Cartilage-on-cartilage stiffening was found to be higher compared to both alumina- and cobalt chromium-on-cartilage stiffening, which were not significantly different from each other. This stiffening response was found to be unique to the superficial zone, as articular loading on cartilage with the superficial zone removed showed no changes in stiffness. The findings of this study suggest that the cartilage superficial zone may adapt its stiffness as a response to articular loading. As the superficial zone is often compromised during the course of osteoarthritic disease, this finding is of clinical relevance, suggesting that the load-bearing function deteriorates over time.

1. Introduction

Articular cartilage is a complex tissue located in diarthrodial joints with heterogenous and biphasic properties. Cartilage contains approximately 60–80% fluid, while the remaining solid phase is comprised of chondrocytes, extracellular matrix, and proteins (Ateshian and Hung, 2006; Mow et al., 1992; Torzilli, 1985). One of the primary functions of articular cartilage is to bear load.

During daily activity, articular cartilage in the knee experiences complex stress patterns at the surface resulting from rolling and sliding motions (Bedi et al., 2013). The knee joint of an active adult undergoes approximately 2 million gait cycles annually, which distributes to about 5480 gait cycles daily (Silva et al., 2002). Understanding the effects of articular loading is crucial, as rolling and sliding as experienced in the knee could have effects on the mechanobiological response of the cartilage. Reports have suggested that specific components of joint kinematics may be related to cartilage thickness changes and potential mechanical risk factors of osteoarthritis development (Favre et al., 2016). Articular loading has been reported to play a role in facilitating biphasic lubrication of the tissue, contributing to the tissue's low coefficient of friction, and stimulating chondrocyte metabolism and mechanotransduction (Ateshian, 2009; Guilak et al., 1995; Moore and Burris, 2017). Although it is well accepted that tissue loading is involved with multiple aspects of tissue health, abnormal tissue loading is also thought to be implicated in cartilage pathology (Chubinskaya and Wimmer, 2013). Methods to investigate complex articular loading on cartilage include *ex vivo* bioreactor systems that mimic joint motion and loading (Wimmer et al., 2004). Such bioreactor systems apply dynamic compression and/or shear on articular cartilage to mechanically stress the tissue (Nugent et al., 2006; Schätti et al., 2016; Trevino et al., 2017). In the past, these systems have been primarily used for measuring biological outputs, and less so to quantify changes in mechanical properties.

Publications from Kempson in the 1970s suggested that the load support function seen in cartilage can be attributed to the tissue's high

* Corresponding author. Yuh Rush University Medical Center, 1611 West Harrison St., Suite 204, Chicago, IL 60612, USA.
E-mail address: catherine_yuh@rush.edu (C. Yuh).

https://doi.org/10.1016/j.jmbbm.2020.104113
Received 30 October 2019; Received in revised form 23 August 2020; Accepted 24 September 2020
Available online 28 September 2020

proteoglycan content, as proteoglycans are highly charged proteins that can draw in fluid through osmotic swelling (Kempson et al., 1970). This has also been demonstrated in recent work using various bath solutions of saline to modulate the swelling capacities of cartilage explants (Nguyen and Levenston, 2012). With fluid influx from osmotic swelling, the collagen fibers also experience high tensile stresses from fluid pressurization (Chahine et al., 2004). As a result, the tissue's stiffness, which may be related to load support function, may vary throughout the tissue depending on proteoglycan content, fluid properties, and collagen structure. While studies have demonstrated that cartilage composition and structure are related to the tissue's stiffness at equilibrium, to our knowledge, no studies have investigated stiffness properties under non-equilibrium conditions as they occur immediately after clinically-relevant joint loading and articulation. Therefore, previous studies do not necessarily capture the effects that occur *in vivo* in the context of complex joint loading. Thus, a baseline understanding of cartilage stiffening during clinically-relevant joint articulation is warranted.

In this study, we present a workflow using a microindenter to obtain measurements of high spatial resolution and mechanical sensitivity of the surface stiffness of cartilage explants before and after joint articulation applied using a tribological bioreactor. This work uniquely brings into context how cartilage responds to the complex loading regimes that occur during gait. While the primary focus is on cartilage-cartilage interactions, we are also interested in the cartilage tissue response after replacing one side of the joint with orthopedic biomaterials such as cobalt-chromium alloy and alumina ceramics as it occurs due to patellar retention in total knee arthroplasty, defect repair, or in hemiarthroplasty, a procedure that is still relevant as an alternative to total arthroplasty in smaller joints such as the shoulder (Custers et al., 2007; Herschel et al., 2017; McCann et al., 2009; Werthel et al., 2018). Previous work from our group has also shown that articular loading on cartilage applied using either a cobalt-chromium alloy and an alumina counterface both led to increased proteoglycan release and Mankin scores compared to cartilage-on-cartilage articular loading (Treviño et al., 2016; Wimmer et al., 2020). Therefore, in the context of this study, it was of interest to investigate how articular loading against various counterface materials, namely cobalt-chromium alloy and alumina, affect cartilage stiffness. Furthermore, we sought to determine whether this response was unique to the top portion of the superficial zone.

The overall aim of this investigation was to assess micron-level stiffness changes at the cartilage surface after articular loading. The specific research questions of this study were: 1) After articular loading, how do factors such as time and counterface material affect cartilage stiffness in the (articulated) contact region and the (non-articulated) non-contact region? 2) Is the stiffness response specific to the superficial zone or a general property of the bulk?

2. Methods

2.1. Tissue harvest and cartilage specimens

Intact bovine stifle joints from twelve 6- to 8-month old steers were obtained from a local abattoir within 48 hr of slaughter and kept refrigerated. Stifle joints were dissected and opened to expose the patellar-femoral trochlear groove. The joint surface was periodically rinsed with 1× PBS throughout the procurement process to maintain hydration of the tissue. The articular cartilage surface was visually examined, where joints that exhibited bruising and/or contact with blood were excluded. Ten joints were frozen intact at −80°C for one freeze-thaw cycle until the day of experiment. Of these ten joints, four were used to assess the effect of counterbody and time on cartilage stiffness before/after bioreactor testing, and six were used to assess the effect of surface removal on cartilage stiffness changes before/after bioreactor testing. These experiments were performed independently of each other. Prior to the day of experiment, frozen joints were thawed at 4°C for 72 hr. In addition to frozen cartilage samples, two fresh joints were used to obtain live cartilage explants for comparison.

During tissue procurement, a 45×8-mm strip was removed from the medial or lateral trochlear rim of each joint using a scalpel. With a custom punch, 14×20-mm oval explants were obtained from the trochlear groove, from areas where the surface was most even in height. All cartilage pieces were trimmed from the underside of the explant to 3-mm thickness using a scalpel. From one stifle joint, a maximum of 6 explants and 2 strips can be obtained (Fig. 1).

2.2. Tribological bioreactor

A bioreactor described in a previous study was used to apply a 40 N compressive load (approximately 2 MPa) and dual-axial articulation (Wimmer et al., 2004). Explants were confined in a porous polyethylene scaffold. Together the explant and scaffold were fit into a dish with 3 mL of lubricant (described below for each experiment). Three different hip ball counterfaces were used to apply articulation against the cartilage explants where noted: 1) a customized ball to which the 45×8×3-mm cartilage strip was attached providing a 32-mm Ø cartilage-on-cartilage articulation 2) a cobalt-chromium 32-mm Ø hip ball for cobalt chromium-on-cartilage articulation and; 3) an alumina 32-mm Ø hip ball for alumina-on-cartilage articulation. Cartilage explants were then loaded, and the applied load was monitored throughout the experiment.

Dual-axial articulation was applied by rotating a hip ball ±15° at 0.5 Hz to apply articulation and rotating the explant ±7.5° at 0.1 Hz and 10 mm offset to apply a 5.4 mm migrating contact using two stepper motors. Static compression was applied using a linear stepper motor.

2.3. Microindentation

A Hysitron TI 950 TriboIndenter (Bruker Inc, Minneapolis, MN) was employed to obtain stiffness measurements. Using a highly sensitive capacitive transducer, displacement-controlled indents were performed on articular cartilage explants that were fully submerged in 1× PBS. A diamond conospherical fluid indenter with a 20-μm radius and 90° cone angle was used during microindentation. Cartilage explants were fixed to a custom sample holder using Loctite® cyanoacrylate glue on the bottom of the explant. An initial measurement of the surface height was performed under dry conditions to prevent false detection due to fluid. Once the surface height within the indenter's local coordinate system was registered, 2.5 mL of 1× PBS were added to fully submerge the explant. An automation using a 1×3 array of 8-μm deep indents, 100-μm apart, was performed. For each indent, a 0.75 μm lift-off phase was first applied, followed by a 10-s loading phase applied at 0.8 μm/s, followed by a 60-s hold phase to account for stress relaxation, followed by an unloading phase applied at −0.8 μm/s. To prevent premature indents that are not in contact with the cartilage surface due to the force detected from only fluid, the setpoint force was adjusted to 7.5 μN to ensure that indenter contact to the surface was achieved. To determine the point of contact, the data was shifted so the origin was located where the load-displacement curve exhibits a sharp increase, indicating contact. Load-displacement data (Fig. 2) were analyzed using the Oliver-Pharr method on the 80–95% portion of the unloading phase (Fig. 2B) (Oliver and Pharr, 2004, 1992). This method calculates the reduced modulus using a power-law fit, which was performed on the beginning of the unloading curve (80–95%). In the context of this study, this material property is referred to as cartilage stiffness, because of its temporal character.

2.4. Bioreactor-indenter workflow

Since it is known that cartilage stiffness varies depending on anatomical region, each explant was measured within the region of articular loading (contact) and in a non-articulated (non-contact) region

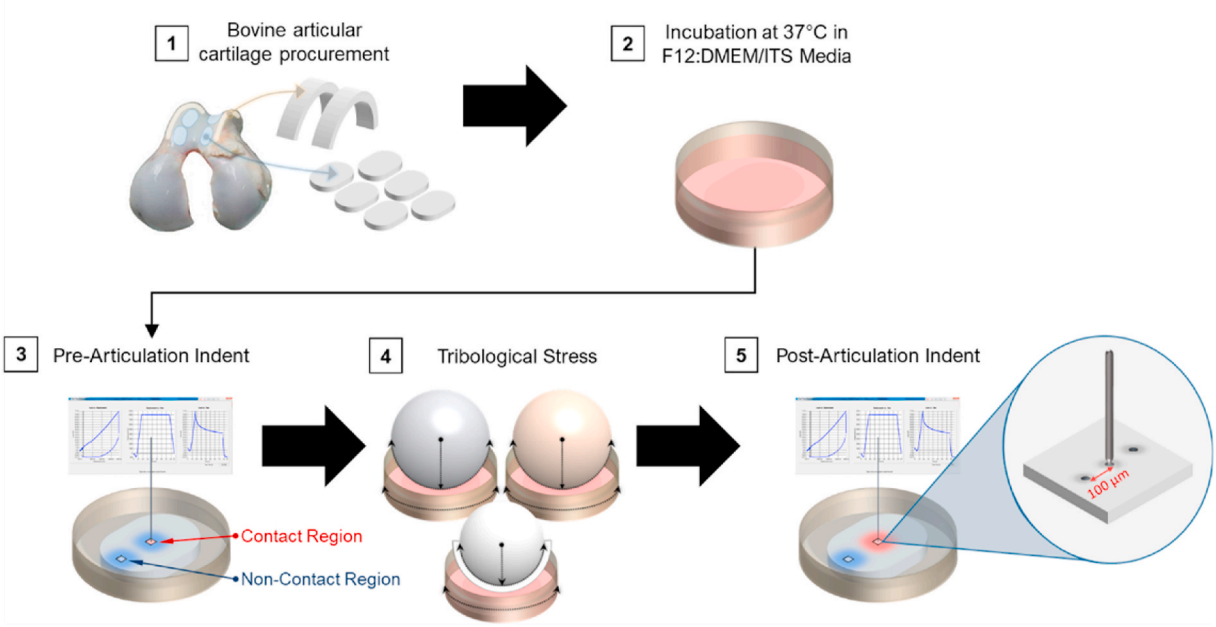

Fig. 1. Bioreactor-indenter workflow used to measure pre- and post-articulation stiffness.

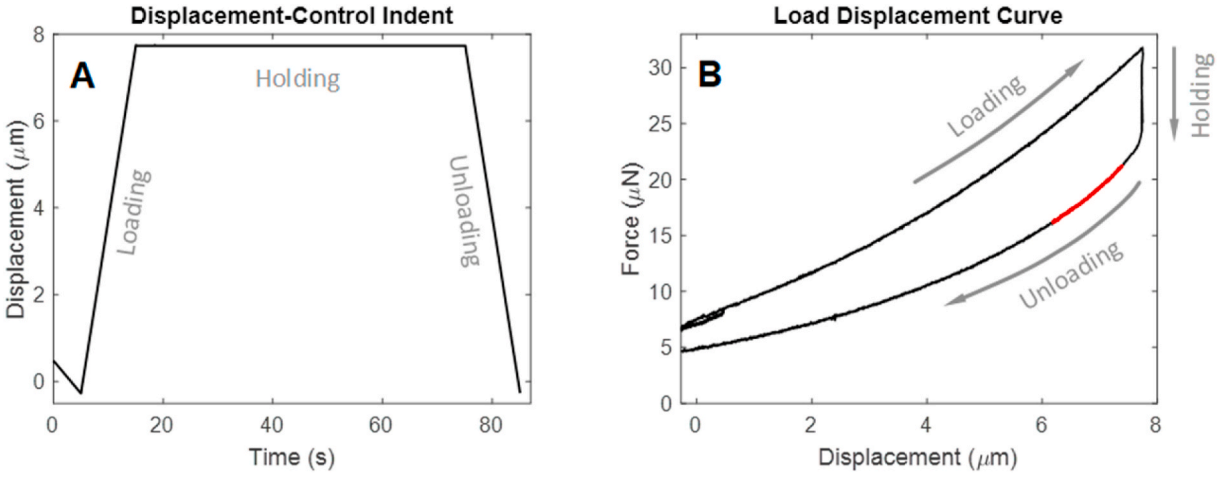

Fig. 2. A) Input displacement applied during indentation; B) Output load-displacement curve obtained during indentation. The region in the unloading phase from which the stiffness is measured is highlighted in red. It is worth noting that the force at the end of the load-displacement curve does not return to the setpoint value of 7.5 μN, indicating relaxation of the tissue during this ~80s indentation protocol.

8 mm left of the contact region. An initial pre-loading indentation was performed for both locations to obtain baseline measurements. Following indentation, cartilage explants were removed from the indentation sample holder and placed into the bioreactor as described earlier. After bioreactor testing, indentation measurements were repeated in both the contact and non-contact regions at 1 hr, 3 hr, 6 hr, and 20 hr post-loading (Fig. 1).

2.5. Time and material dependence of stiffening effect

Twelve explants were obtained from four freeze-thawed joints (three explants per joint, four animals) and used to assess cartilage stiffness changes over time and the effect of the counterbody material. From each joint, one freeze-thawed explant was tested per day. Explants from the same joint were distributed into three groups based on counterface: 1) cartilage; 2) cobalt-chromium and; 3) alumina, resulting in four replicates per condition (n=4). DMEM/F12 culture media was used as the lubricant and articular loading was applied for 3 hr, or 5400 gait cycles, comparable to the average number of cycles a human adult experiences daily (Silva et al., 2002). Experiments were executed at 37°C in >85% humidity.

To verify that the observed effects are not an artifact due to tissue handling (i.e. freeze-thawing), two live cartilage explants from two freshly obtained joints (n=2) were placed in DMEM/F12 culture media, and placed into an incubator at 37°C, 5% CO_2 for a three-day preculture period, with daily media changes to maintain cell viability above 80%. Following preculture, the bioreactor-indenter workflow described above was performed on these explants using a cartilage-on-cartilage interface. Indentation was performed both before and 1 hr after bioreactor testing.

2.6. Surface effect of cartilage stiffening

For this particular question, we procured twenty-four explants from six freeze-thawed joints (six animals) and distributed them into four groups per animal: 1) surface intact, articulated, 2) surface intact, free swelling control (FSC); 3) surface removed, articulated and; 4) surface

removed, FSC, resulting in six replicates per condition (n=6). Following explant preparation, on Day 2, a vibratome (Vibratome® Series 3000) was employed to remove 500 μm off the surface in the surface removed groups. Explants were fixed to a vibratome sample holder using cyanoacrylate super glue, and surface removal was performed submerged in 1× PBS to maintain tissue hydration. Following surface removal, explants were placed in fresh 1× PBS at 4°C overnight. A complete removal of the superficial zone in the contact region was histologically verified. Because of the tissue's inherent curvature, 500 μm of surface removal was only applied for the contact region; no indentation measurements on the non-contact region of the tissue were performed. On Day 3, the bioreactor-indenter workflow described earlier was applied to the explants using 1× PBS as the lubricant and for 1 hr of articular loading with an alumina counterface.

2.7. Data analyses

The cartilage stiffness values (kPa) used in analyses were the average of the 3 values in the 1x3 indentation array. This allowed us to use a randomized complete block design (RCBD) mixed model to assess each of the experiments performed in this study, where our separate "blocks" (in this case each animal used) can be represented as a random factor in our model (Dixon, 2016). Each of the blocks contains a complete set of experimental treatments, where the number of blocks and experimental treatments are the same. All analyses were performed using Design--Expert® Software Version 11 and SPSS 22. For reference, the significance level was set at p=0.05. Power analyses were performed for all experiments to ensure a power of at least 0.8 at a significance level of 0.05, which are detailed in the following paragraphs.

The effect on cartilage surface stiffness of 1) location on explant (contact region, non-contact region), 2) time (pre-, post-1hr, post-3hr, post-6hr, post-20hr), and 3) counterface material (cartilage, cobalt-chromium, alumina), was analyzed using a three-way ANOVA with four replicates (n=4). The ANOVA was blocked relative to the four animals (b=4) used in the experiments, with one block per replicate, resulting in a RCBD. The ANOVA analysis yielded a regression model that was used to assess the effect of specific factor levels on surface stiffness, such as the stiffness versus time for each counterface. With four replicates, it was expected that effects of 0.52, 1.0, and 0.71 standard deviations (SD) would be detectable for location, time, and material, respectively, with a power of 0.8 at a significance level of 0.05. These effect sizes correspond to detecting differences of approximately 104 kPa, 200 kPa, and 142 kPa due to location, time, and material, respectively, or of 37%, 71%, and 51%, respectively. Comparisons of these data to fresh tissue explants undergoing cartilage-on-cartilage articular loading were performed using pairwise comparisons.

For the surface removal experiments (n=6), the stiffness data were analyzed using an animal-blocked (b=6), RCBD two-way ANOVA to assess the effect of 1) load (loaded vs. FSC), and 2) surface removal (surface-intact vs. surface-removal). Two ANOVA analyses were conducted: one on the cartilage stiffness values and another on the stiffness values normalized to (divided by) the pre-test cartilage stiffness values. With six replicates, an effect size of 1.22 SD or greater associated with load and/or surface removal should be detectable with a power of 0.8 at a significance level of 0.05. Given a representative SD of 50 kPa for these experiments, this effect size corresponds to being able to detect an effect of 61 kPa or greater stemming from any of these factors.

Post-hoc pairwise comparisons were performed using t-tests to compare individual groups, such as the cartilage surface stiffness in the contact area versus that in the non-contact area post-1hr, or to compare the effect of the counterface materials on cartilage stiffness. Unless otherwise stated, the p-values quoted in the text were obtained from t-tests. Additionally, Shapiro-Wilks tests for normality of the normalized values were performed.

3. Results

The 3-way ANOVA model for the combined effect of location, time, and counterface material on the surface stiffness of the freeze-thawed cartilage samples was found to be statistically highly significant (p<0.0001), in association with the significant effect of time (p=0.0030), its interaction with location (p=0.0002), and the effect of material (p=0.0015) (Table 1). The model clearly shows transient stiffening of the cartilage surface in the contact area at post-1hr (Fig. 3), consistent with the significant time and time-location effects. The significant counterface material effect corresponds to the greater average stiffness obtained with cartilage-on-cartilage versus cartilage against cobalt-chromium and alumina.

3.1. Cartilage-on-Cartilage articular loading effect on cartilage stiffness

Baseline measurements of cartilage stiffness in the contact and non-contact regions for cartilage-on-cartilage articular loading indicated no significant differences between the contact and non-contact regions prior to bioreactor testing (p=0.30). In the post-loading assessment, 1 hr following the end of articular loading, cartilage stiffness was shown to be significantly increased in the contact region compared to baseline (p<0.0001). In contrast, non-contact regions exhibited no significant changes in stiffness compared with baseline at the 1 hr time point (p=0.88). At 3 hr post-loading and later, the average stiffness in the articulated region was shown to have decreased towards baseline (p=0.33) and resembled values of the non-articulated region (p=0.69).

3.2. Counterbody material effect on cartilage stiffening

The effect of material was shown to be highly significant (p=0.0015). Post-hoc assessment indicated that all three counterbody materials showed significantly higher stiffness at the 1 hr time point in the contact region compared to the non-contact region (Fig. 4) (p<0.05 for all materials). To visualize relative stiffness changes (Fig. 5), the stiffness measurements were normalized to the stiffening response (post/pre-articulation) and the specific sample (contact/non-contact) (Equation 1).

$$\left(\frac{\text{Post}}{\text{Pre}}\right)_{\text{Contact}} \Big/ \left(\frac{\text{Post}}{\text{Pre}}\right)_{\text{Non-Contact}} \quad (1)$$

3.3. Cartilage stiffness changes after articular loading in live tissue

Similar to the freeze-thawed explants presented in section 3.1, an RCBD ANOVA model assessing the cartilage stiffness response in live tissue was shown to be highly significant (p=0.006). Live explants were shown to have a significant increase in stiffness in the contact region compared to the non-contact region (p<0.001). Similar to freeze-thawed tissues, no significant differences were found between the baseline pre-loading cartilage stiffness values in the contact and non-contact regions (p=0.58), and between the pre- and post-loading stiffness values in the non-contact region (p=0.94) (Fig. 6). Overall, the relative stiffness

Table 1
Probability values for the 3-way ANOVA model on the effect of counterbody material, location, and time on cartilage surface stiffness.

Variable	p-value
ANOVA Model	<0.0001
Time	0.0030
Location	0.1189
Material	0.0015
Time-Location	0.0002
Time-Material	0.1518
Location-Material	0.8078

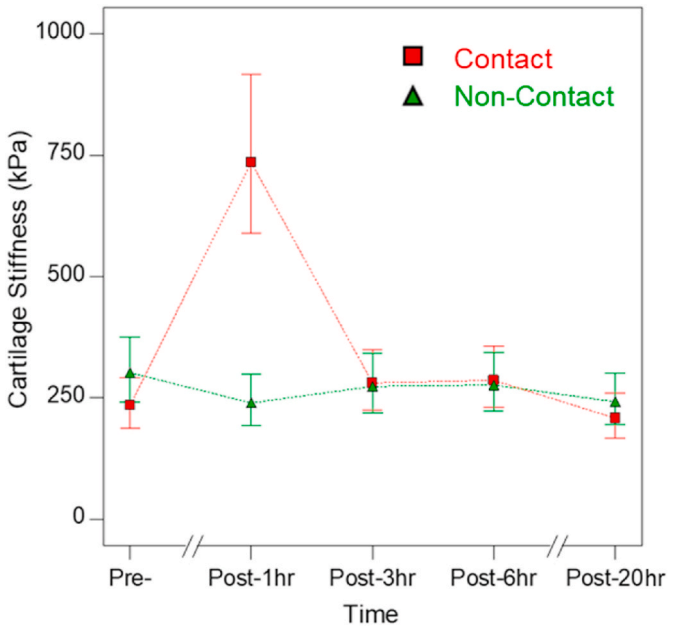

Fig. 3. Surface stiffness of the freeze-thawed cartilage as a function of time point in the contact location (red squares) and the non-contact location (green triangles), averaged over the three counterface materials (cartilage, cobalt-chromium alloy, and alumina). The effect of counterbody material is presented in Section 3.2. Data (n=4, N=120) is presented as the regression Mean ± Least Significant Difference (LSD) 95% Confidence Intervals.

change of fresh tissue followed that of freeze-thawed tissue leading to a 5.68 ± 0.19 (mean ± SEM) stiffness increase at the 1 hr time point, a value which is close to 7.38 ± 1.79 for freeze-thawed tissue.

3.4. Surface removal effect on cartilage stiffening

The 2-way ANOVA regression model for the effect of surface removal and tribological loading on cartilage surface stiffness was statistically highly significant (p=0.0042), with a significant load–surface removal interaction term (p=0.0115). This term arises because only the explants with an intact surface experienced stiffening with tribological loading (Fig. 7). This difference in behavior is even more clearly visible in a 2-way ANOVA model of the normalized (post/pre-test ratio) stiffness values (p=0.0006, Table 2).

For this dataset, only contact region tissue stiffnesses were assessed. From post-hoc pairwise comparisons, it was found that prior to bioreactor testing, surface-removed cartilage explants exhibited significantly higher (p<0.001) tissue stiffness values compared to animal-matched surface-intact explants. Thus, as expected, the underlying middle zone exhibited higher stiffness values compared to the superficial zone at baseline (Schinagl et al., 1996; Wang et al., 2001). For the intact surface groups, loaded explants exhibited a significantly increased stiffening response following articular loading compared to the FSC explants, as expected (p=0.006). For the removed surface groups, there was no significant difference between loaded and FSC explants (p=0.927). When comparing loaded groups, the intact surface group had a significantly higher stiffening response compared to the removed surface group (p=0.013) (Fig. 7).

4. Discussion

With the advent of higher spatial resolution mechanical testing

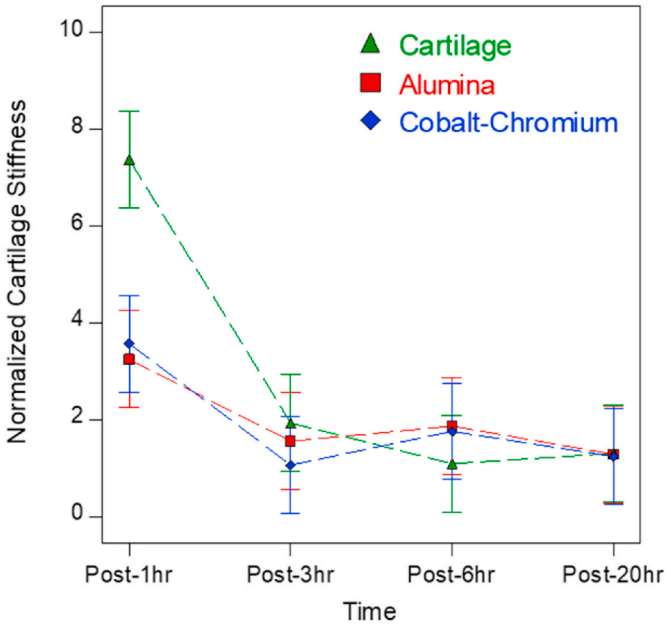

Fig. 5. Relative stiffness changes (determined by Equation 1) of each post-loading time group and each material for freeze-thawed cartilage. As observed from this visualization, at the 1 hr time point, the stiffness ratio of the cartilage counterface group is higher compared to the alumina and cobalt-chromium groups. Data (n=4) is presented as Mean ± LSD 95% Confidence Intervals.

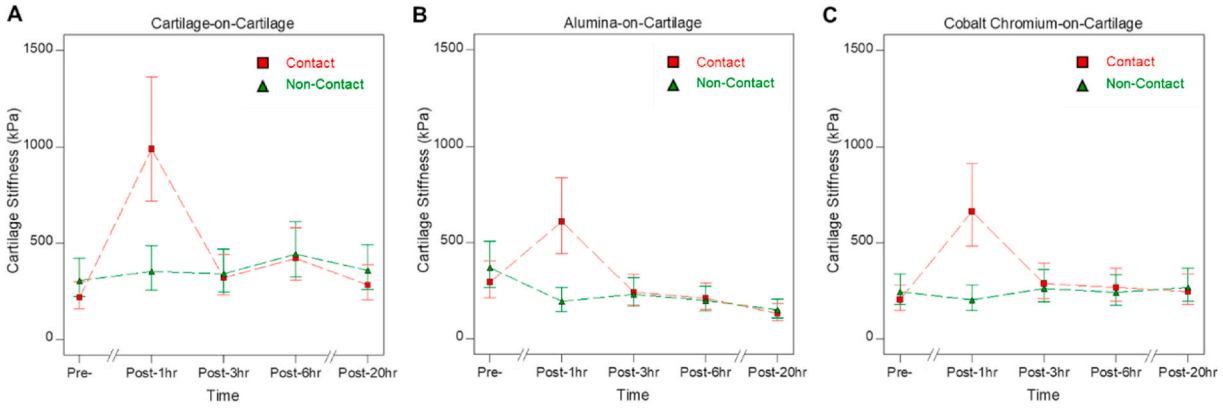

Fig. 4. Interaction plots of the counterbody material-time interaction for A) Cartilage-on-Cartilage, B) Alumina-on-Cartilage, and C) Cobalt Chromium-on-Cartilage. The contact and non-contact region cartilage stiffnesses for each material group is shown over time from end of articular loading. Data (n=4) is presented as Mean ± LSD 95% Confidence Intervals.

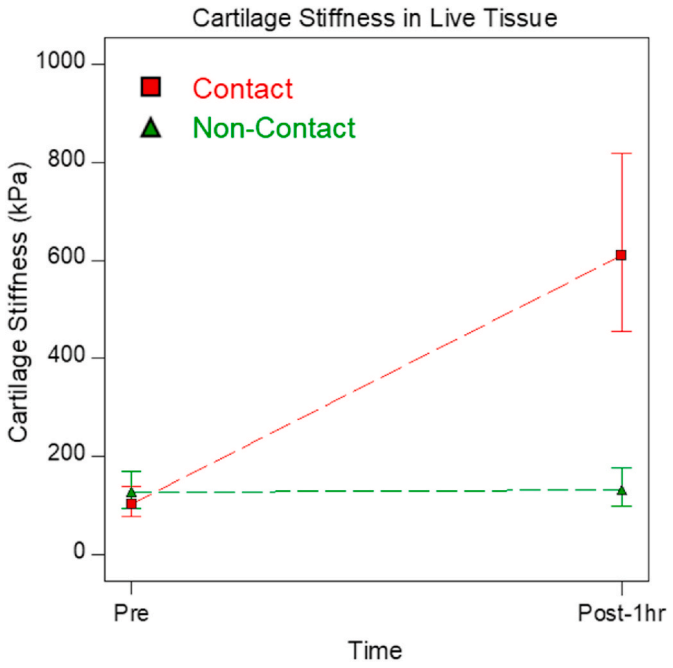

Fig. 6. Interaction plot showing the effect of cartilage-on-cartilage articular loading on cartilage stiffness on live cartilage explants (n=2). The cartilage stiffening that was observed in articulated freeze-thawed explants (shown above) was also observed in articulated live tissue. The horizontal green interaction line, representing the non-contact region, shows no change in stiffness before and after bioreactor testing. The sloped red interaction line, representing the contact region, indicates a stiffening response after applied articular load. Data (n=2) is presented as Mean ± LSD 95% Confidence Intervals.

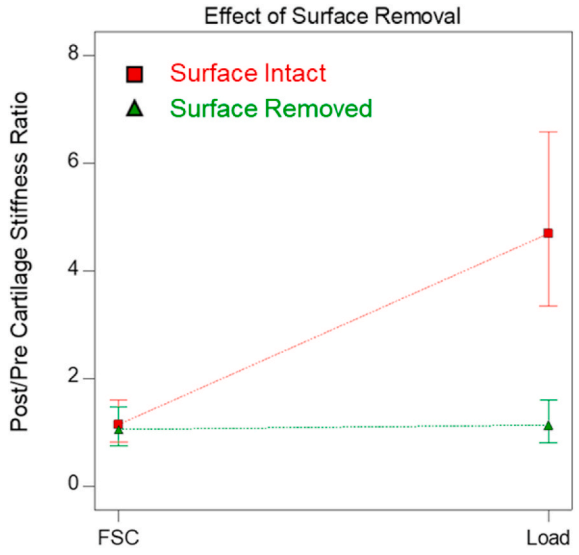

Fig. 7. Interaction plot of 2-way ANOVAs for the effect of surface removal in conjunction with articular loading on surface stiffness of cartilage explants, presented in terms of normalized (post/pre-test ratio) cartilage stiffness. The horizontal green interaction line indicates that for explants with a removed surface, no significant difference exists between the FSC and Load groups. In contrast, the sloped red interaction line demonstrates that for intact cartilage, tissue stiffness remains the same in the FSC condition and increases when load is applied. Data (n=6, N=24) is presented as the regression Mean ± LSD 95% Confidence Intervals.

Table 2
Probability values for the 2-way ANOVA models on the effect of surface removal and tribological loading on cartilage surface stiffness. The resulting models are shown graphically in Fig. 7.

Variable	p-value
ANOVA Model	0.0006
Load	0.0048
Surface Removal	0.0045
Load-Surface Removal	0.0095

methods, such as micro- and nanoindentation, it has become possible to study the surface mechanical properties of articular cartilage. While articular cartilage microindentation studies have been performed (McGann et al., 2014; Moshtagh et al., 2018; Wahlquist et al., 2017), to the best knowledge of the authors, there has been no study that investigates cartilage stiffness changes after tribological challenge of the tissue. Therefore, the goal of this study was to determine longitudinal changes in surface stiffness due to combined compressive load and articulation as occurs in the knee joint during gait.

The results of this study demonstrate that articular loading leads to an immediate increase in cartilage stiffness at the surface. Only the cartilage within the contact path experienced stiffening, while non-contact regions outside of the contact path remained unaffected. This stiffening effect is also transient, as the tissue had returned to baseline stiffness within 3 hr post-articular loading. The results also showed that the choice of counterface material matters: cartilage-on-cartilage led to higher stiffening than artificial materials after articular loading. The adaptive stiffening of the cartilage surface following articular loading may demonstrate the tissue's ability to optimize its properties to a specific mechanical input. It may vary with the specific joint load and contact path (and thus activity). Interestingly, after removal of the surface the stiffening response due to articular loading is lost, suggesting that stiffening is a phenomenon of the topmost region of the superficial zone.

Historically, cartilage stiffness changes in the context of osteoarthritis has indicated tissue softening and not stiffening (Kempson et al., 1970; Treviño et al., 2016; Waldstein et al., 2016). Yet, stiffening of cartilage has been observed in the context of nanoindentation during dehydration of the tissue (Boettcher et al., 2016; Han et al., 2018), as well as clinically with the formation of advanced glycation end products (AGEs) with age (Chen et al., 2002; McGann et al., 2014; Moshtagh et al., 2018; Verzijl et al., 2002). Specifically, AGEs induce the formation of covalent bonds of the collagen network, and as the stiffening response observed in this study was transient, it is unlikely that the stiffening mechanism following articular loading is due to AGEs-induced crosslinks.

The stiffening effect observed may also be related to the topmost surface structure of the tissue. Previously, using phase-contrast microscopy, this topmost zone has been identified as the *lamina splendens* due to its particular appearance (MacConaill, 1951). Environmental scanning electron microscopy, extended surface forces apparatus, and atomic force microscopy images have revealed an amorphous (gel-like) zone on the surface of approximately ~4 μm thickness (Crockett et al., 2005; Shoaib and Yuh et al., 2020). The boundary zone contains hyaluronan, glycoproteins, and phospholipids, likely adsorbed onto the cartilage from the synovial fluid (Crockett et al., 2007). Lubricin, one of the glycoproteins in the boundary zone, can form a negatively-charged brush-like structure that provides repulsion between opposing surfaces in an aqueous environment (Zappone et al., 2007). Based on this brush-like structure theory, one potential mechanism of cartilage stiffening could be that these brushes "flatten" during articular loading in the contact area. Nevertheless, lubricin can stretch at most ~200 nm (its length), and hence, the boundary zone indented here (8 μm) cannot be solely composed of this brush-like structure (Swann et al., 1981;

Zappone et al., 2007). It has been hypothesized by Crockett et al. that hydrophobic bonds between the phospholipids and glycoproteins or hyaluronan within the amorphous gel-like zone may be forced to form upon compression, during which fluid exudation occurs, thereby leading to a transient change of the structure (Crockett et al., 2007). It is therefore possible that the flattened brush and the collapsed surface gel-like layer justify the observed increase in stiffness of the upper region of the superficial zone that is measured in these microindentation experiments.

In addition, collagen binding molecules may play a role in the stiffening response by forming molecular complexes. According to Heinegård and Saxne, collagen fibers can be crosslinked through binding interactions of COMP, collagen IX, decorin, and matrilin-3 (Heinegård and Saxne, 2010). Heinegård's work suggested that complexes of these molecules are formed in order to bind collagen fibers. Therefore, it is possible that, as fluid is exuded during articular loading in the contact region, compression of the solid matrix decreases the proximity between collagen fibers in the superficial zone, potentially enhancing temporary crosslinking of these molecules between fibers. As these molecules bind the fibers, it may provide stabilization to the fibrillar network that manifests as micro-scale stiffening following articular loading. Such a mechanism has been described by Nagel and Kelly (2013). In their model, crosslinked collagen fibers were shown to be recruited earlier when the network is stretched compared to fibers that are not crosslinked, which led to an increase in stiffness.

A third potential mechanism behind tribologically-induced stiffening may be related to the tensioning of the parallel collagen fibers in the superficial zone. Tensioning of these fibers may occur due to the buildup of fluid pressure in the contact region, as a highly pressurized convergence wedge develops on the edge of the region during sliding (Moore and Burris, 2017, 2014). Increased fluid pressure in the contact may lead to an increase of tension of the fibers and, thus, a decrease of their compliance to axial loading (Chahine et al., 2004).

In the short-term experiments of this study, it was found that the cartilage groups that underwent rigid-on-cartilage articular loading still exhibited stiffening, albeit less compared to the cartilage-on-cartilage groups. The effect of stiffening was largest for the cartilage-cartilage contact (7×), while both cobalt-chromium and alumina contact only stiffened the cartilage surface to approximately half of this value. This may be related to competing effects of surface damage and adjustment. In the tissue's hydrated state, the charge of biological macromolecules within the boundary zone may be screened by the ions present in the aqueous phase (from the lubricant). However, the decrease in water content leads to a concurrent increase in charge density within the boundary zone, which may enhance the electrostatic repulsion at the interface. When the load is removed, the rehydration of the boundary layer progresses as time passes, and the gel-like structure may be allowed to reform, explaining the transient nature of the response observed. Previous work from our group has shown that articular loading applied using a cobalt-chromium counterface leads to a higher amount of proteoglycan release compared to cartilage-on-cartilage articular loading (Treviño et al., 2016). Similar observations have been made with alumina counterfaces (Wimmer et al., 2020). Thus, loading such artificial materials against cartilage may compromise the gel-like layer, and with the release of charged proteoglycans from the boundary zone, a reduction of repulsion within the interface may occur. This could therefore further justify the more prominent stiffening observed in the cartilage-on-cartilage articular loading group compared to alumina-on-cartilage or cobalt chromium-on-cartilage groups.

Although reports of microindentation of cartilage have increased significantly over the past decade, one of the challenges of this field is the determination of the appropriate analysis method. In this study, because it was specifically of interest to measure the cartilage response immediately after loading and articulation, the tissue stiffness was measured in non-equilibrium conditions. In order to mitigate nonlinear effects, we applied the same indentation depth and identical relaxation times throughout testing, thus providing grounds for stiffness comparison. In order to better control for changing conditions due to articulation, we took measurements inside *and* outside the contact zone on the same tissue samples. The Oliver Pharr method was chosen for this study due to its simplicity. The Oliver Pharr method has been applied for indentation of materials that have nonlinear unloading curves and has been widely used in cartilage indentation in the literature (Gupta et al., 2005; McGann et al., 2014; Moshtagh et al., 2018). This method has also been described to be useful in determining trends of cartilage stiffness as a result of experimental testing conditions (Han et al., 2011). Furthermore, using a small spherical indenter made of diamond, we did not observe adhesion, an artifact that has been reported for larger indenter sizes that can lead to overestimation of tissue stiffness in the indentation analysis using the Oliver-Pharr method (Kohn and Ebenstein, 2013).

However, it is crucial to note that the Oliver Pharr method can only assess the solid contributions to stiffness and does not provide time-dependent properties of the tissue. Therefore, a limitation of the presented study is that by using the Oliver Pharr method, the fluid fraction contribution to the stiffness behavior observed is not captured. Alternative models of analysis have been recently developed that incorporate nonlinear biphasic and poroelastic parameters that are more representative of the time-dependent properties in articular cartilage (Moore and Burris, 2014; Oyen, 2013). However, the assumptions of these complex analysis models are not met in our study, as we indent the tissue immediately after articular loading when it is driven out of equilibrium. The fluid's contribution to tissue stiffness during compressive load has been widely investigated, and therefore, it is thought that stiffness is attributed to fluid pressurization in cartilage (Ateshian, 2009; Ateshian et al., 1994; Bachrach et al., 1998; Mow et al., 1980; Spilker et al., 1990). More recently, increasing evidence has also shown that sliding leads to tribological rehydration at the surface of the tissue (Burris et al., 2019; Graham et al., 2018). Such a mechanism could have implications on the stiffness of the top-most gel-like layer (Lin et al., 2020; Raviv and Klein, 2002; Shoaib and Yuh et al., 2020). While it has been shown that fluid is a driver of stiffness behavior in cartilage, it has also been extensively reported that alterations to the solid matrix can change the stiffness behavior of the tissue (Basalo et al., 2004; Hosseini et al., 2013; Khoshgoftar et al., 2018; McGann et al., 2014; Moshtagh et al., 2018; Waldstein et al., 2016). Changes of the solid phase can also have major implications in the context of osteoarthritis, as it is the specifically the solid matrix that degrades. Nonetheless, in the future, it will be important to explore time-dependent analyses methods to capture the fluid's contribution as well.

There are additional limitations of this investigation. One of the challenges was that the duration of each bioreactor-indenter workflow experiment for each explant had to be performed individually over several hours per day. Therefore, freeze-thawed tissue samples were used to assess the transient stiffening response after 3 hr of loading. Three hours was chosen because the number of cycles approximately represents the daily walking cycles of an adult. Unlike the time-/material-dependence experiments, all four groups of surface removal explants were performed within one day to minimize experimental artifacts that could occur over performing separate independent experiments on different days. This was only possible by reducing the time of articular loading to 1 hr. Even with this low loading duration, the stiffening response was still observed in these experiments. Further, it is also important to note that the lubricants between the time-/material-dependence experiments and surface removal experiments were different. During surface removal, a large volume (>150 mL) of 1× PBS had to be used as the bath solution since the lubricant is colorless and clear, allowing the surface removal process to be better observed to increase precision. Because the explants in the surface removal study were placed in 1× PBS during surface removal, 1× PBS was also used during bioreactor testing as the bath solution instead of culture media to maintain consistency. The normalization performed in the surface removal studies also did not include the non-contact region, as this

region was not measured due to the convexity of the tissue, as mentioned above. Finally, it is important to note that the tissue source used for this study was juvenile bovine cartilage. Thus, the stiffening response observed in these findings is a feature of young cartilage and has to be confirmed for adult tissue.

In future work, the time-dependent stiffening response will be investigated between 1 and 3 hr post-articulated in smaller time increments to assess the rate at which cartilage stiffness decreases towards pre-articulated values. Additionally, the mechanism(s) behind the findings of this study will be investigated, such as assessing the potential role of biochemical constituents and/or lubrication parameters in cartilage stiffening.

5. Conclusion

In this investigation, cartilage stiffness at the surface was assessed immediately following tribological challenge. The results of this study demonstrated that the cartilage surface transiently stiffens as a result of articular loading. It was also found that using a cartilage-on-cartilage interface led to higher stiffening compared to using artificial counterface materials. This stiffening response was also shown to be a unique feature of the superficial zone, as surface removal attenuated this response. Cartilage stiffness is a mechanical indicator of cartilage health and has been reported to decrease in pathological tissue (Broom and Flachsmann, 2003; Hosseini et al., 2013; Waldstein et al., 2016). As one of cartilage's primary functions is to bear load, tissue stiffness may be involved in sustaining the tissue's resistance to over-loading, thereby preventing damage to the tissue. The findings of this study suggest that the cartilage surface may adapt its stiffness as a response to mechanical loading, and this adaptive stiffening may compete with wear-induced softening. The loss of stiffening response when the superficial zone is removed may indicate a loss of load bearing function, which may also have implications in osteoarthritic cartilage where this layer is compromised. Finally, the bioreactor-indenter workflow presented in this study can be expanded to provide additional perspectives on the link between changes in surface stiffness and biochemical constituents due to cartilage articular loading.

Funding

This work was supported by the National Institutes of Health R01 AR066635 (S.C. and M.W.) and National Science Foundation Grant No. 17–61696 (R.M.E.M).

CRediT authorship contribution statement

Yuh C: Study design, Methodology, Validation, Investigation, Formal analysis, Data curation, Writing - original draft, Visualization. **M.P. Laurent:** Study design, Formal analysis, Writing - review & editing. **R.M. Espinosa-Marzal:** Methodology, Writing - review & editing. **S. Chubinskaya:** Study design, Funding acquisition, Writing - review & editing. **M.A. Wimmer:** Conceptualization, Supervision, Funding acquisition, Resources, Writing - review & editing.

Declaration of competing interest

The authors declare that they have no known competing financial interests or personal relationships that could have appeared to influence the work reported in this paper.

Acknowledgements

The authors thank Dr. Kristin Al-Ghoul and John Gallagher for lending us the Vibratome used in this study, Arnavaz Hakimiyan for histological assistance, Dr. Lou Fogg and Jade He for discussion on statistical design, Dr. Thomas Nagel and Dr. Steven Mell for helpful discussion and review of the manuscript, and our funding sources.

References

Ateshian, G.A., 2009. The role of interstitial fluid pressurization in articular cartilage lubrication. J. Biomech. 42, 1163–1176. https://doi.org/10.1016/j.jbiomech.2009.04.040.

Ateshian, G.A., Hung, C.T., 2006. The natural synovial joint: properties of cartilage. Proc. Inst. Mech. Eng. Part J. Eng. Tribol. 220, 657–670. https://doi.org/10.1243/13506501JET86.

Ateshian, G.A., Lai, W.M., Zhu, W.B., Mow, V.C., 1994. An asymptotic solution for the contact of two biphasic cartilage layers. J. Biomech. 27, 1347–1360. https://doi.org/10.1016/0021-9290(94)90044-2.

Bachrach, N.M., Mow, V.C., Guilak, F., 1998. Incompressibility of the solid matrix of articular cartilage under high hydrostatic pressures. J. Biomech. 31, 445–451. https://doi.org/10.1016/S0021-9290(98)00035-9.

Bedi, A., Chen, T., Santner, T.J., El-Amin, S., Kelly, N.H., Warren, R.F., Maher, S.A., 2013. Changes in dynamic medial tibiofemoral contact mechanics and kinematics after injury of the anterior cruciate ligament: a cadaveric model. Proc. Inst. Mech. Eng. [H] 227, 1027–1037. https://doi.org/10.1177/0954411913490387.

Boettcher, K., Kienle, S., Nachtsheim, J., Burgkart, R., Hugel, T., Lieleg, O., 2016. The structure and mechanical properties of articular cartilage are highly resilient towards transient dehydration. Acta Biomater. 29, 180–187. https://doi.org/10.1016/j.actbio.2015.09.034.

Broom, N.D., Flachsmann, R., 2003. Physical indicators of cartilage health: the relevance of compliance, thickness, swelling and fibrillar texture. J. Anat. 202, 481–494. https://doi.org/10.1046/j.1469-7580.2003.00184.x.

Burris, D.L., Ramsey, L., Graham, B.T., Price, C., Moore, A.C., 2019. How sliding and hydrodynamics contribute to articular cartilage fluid and lubrication recovery. Tribol. Lett. 67, 46.

Chahine, N.O., Wang, C.C.-B., Hung, C.T., Ateshian, G.A., 2004. Anisotropic strain-dependent material properties of bovine articular cartilage in the transitional range from tension to compression. J. Biomech. 37, 1251. https://doi.org/10.1016/j.jbiomech.2003.12.008.

Chen, A.C., Temple, M.M., Ng, D.M., Verzijl, N., DeGroot, J., TeKoppele, J.M., Sah, R.L., 2002. Induction of advanced glycation end products and alterations of the tensile properties of articular cartilage. Arthritis Rheum. 46, 3212–3217. https://doi.org/10.1002/art.10627.

Chubinskaya, S., Wimmer, M.A., 2013. Key pathways to prevent posttraumatic arthritis for future molecule-based therapy. Cartilage 4, 13S–21S. https://doi.org/10.1177/1947603513487457.

Crockett, R., Grubelnik, A., Roos, S., Dora, C., Born, W., Troxler, H., 2007. Biochemical composition of the superficial layer of articular cartilage. J. Biomed. Mater. Res. 82, 958–964. https://doi.org/10.1002/jbm.a.31248.

Crockett, R., Roos, S., Rossbach, P., Dora, C., Born, W., Troxler, H., 2005. Imaging of the surface of human and bovine articular cartilage with ESEM and AFM. Tribol. Lett. 19, 311–317. https://doi.org/10.1007/s11249-005-7448-2.

Custers, R.J.H., Dhert, W.J.A., van Rijen, M.H.P., Verbout, A.J., Creemers, L.B., Saris, D.B.F., 2007. Articular damage caused by metal plugs in a rabbit model for treatment of localized cartilage defects. Osteoarthritis Cartilage 15, 937–945. https://doi.org/10.1016/j.joca.2007.02.007.

Dixon, P., 2016. Should blocks be fixed or random? 2016 Conference on Applied Statistics in Agriculture Proceedings 23–39. https://doi.org/10.4148/2475-7772.1474.

Favre, J., Erhart-Hledik, J.C., Chehab, E.F., Andriacchi, T.P., 2016. Baseline ambulatory knee kinematics are associated with changes in cartilage thickness in osteoarthritic patients over 5 years. J. Biomech. 49, 1859–1864. https://doi.org/10.1016/j.jbiomech.2016.04.029.

Graham, B.T., Moore, A.C., Burris, D.L., Price, C., 2018. Mapping the spatiotemporal evolution of solute transport in articular cartilage explants reveals how cartilage recovers fluid within the contact area during sliding. J. Biomech. 71, 271–276. https://doi.org/10.1016/j.jbiomech.2018.01.041.

Guilak, F., Ratcliffe, A., Mow, V.C., 1995. Chondrocyte deformation and local tissue strain in articular cartilage: a confocal microscopy study. J. Orthop. Res. Off. Publ. Orthop. Res. Soc. 13, 410–421. https://doi.org/10.1002/jor.1100130315.

Gupta, H.S., Schratter, S., Tesch, W., Roschger, P., Berzlanovich, A., Schoeberl, T., Klaushofer, K., Fratzl, P., 2005. Two different correlations between nanoindentation modulus and mineral content in the bone-cartilage interface. J. Struct. Biol. 149, 138–148. https://doi.org/10.1016/j.jsb.2004.10.010.

Han, G., Hess, C., Eriten, M., Henak, C.R., 2018. Uncoupled poroelastic and intrinsic viscoelastic dissipation in cartilage. J. Mech. Behav. Biomed. Mater. 84, 28–34. https://doi.org/10.1016/j.jmbbm.2018.04.024.

Han, L., Grodzinsky, A.J., Ortiz, C., 2011. Nanomechanics of the cartilage extracellular matrix. Annu. Rev. Mater. Res. 41, 133–168. https://doi.org/10.1146/annurev-matsci-062910-100431.

Heinegård, D., Saxne, T., 2010. The role of the cartilage matrix in osteoarthritis. Nat. Rev. Rheumatol. 7 https://doi.org/10.1038/nrrheum.2010.198 nrrheum.2010.198.

Herschel, R., Wieser, K., Morrey, M.E., Ramos, C.H., Gerber, C., Meyer, D.C., 2017. Risk factors for glenoid erosion in patients with shoulder hemiarthroplasty: an analysis of 118 cases. J. Shoulder Elbow Surg. 26, 246–252. https://doi.org/10.1016/j.jse.2016.06.004.

Hosseini, S.M., Veldink, M.B., Ito, K., van Donkelaar, C.C., 2013. Is collagen fiber damage the cause of early softening in articular cartilage? Osteoarthritis Cartilage 21, 136–143. https://doi.org/10.1016/j.joca.2012.09.002.

Kempson, G.E., Muir, H., Swanson, S.A.V., Freeman, M.A.R., 1970. Correlations between stiffness and the chemical constituents of cartilage on the human femoral head. Biochim. Biophys. Acta BBA - Gen. Subj. 215, 70–77. https://doi.org/10.1016/0304-4165(70)90388-0.

Kohn, J.C., Ebenstein, D.M., 2013. Eliminating adhesion errors in nanoindentation of compliant polymers and hydrogels. J. Mech. Behav. Biomed. Mater. 20, 316–326. https://doi.org/10.1016/j.jmbbm.2013.02.002.

Lin, W., Liu, Z., Kampf, N., Klein, J., 2020. The role of hyaluronic acid in cartilage boundary lubrication. Cells 9, 1606. https://doi.org/10.3390/cells9071606.

MacConaill, M.A., 1951. The movements of bones and joints; the mechanical structure of articulating cartilage. J. Bone Joint Surg. Br. 33B, 251–257.

McCann, L., Ingham, E., Jin, Z., Fisher, J., 2009. An investigation of the effect of conformity of knee hemiarthroplasty designs on contact stress, friction and degeneration of articular cartilage: a tribological study. J. Biomech. 42, 1326–1331. https://doi.org/10.1016/j.jbiomech.2009.03.028.

McGann, M.E., Bonitsky, C.M., Ovaert, T.C., Wagner, D.R., 2014. The effect of collagen crosslinking on the biphasic poroviscoelastic cartilage properties determined from a semi-automated microindentation protocol for stress relaxation. J. Mech. Behav. Biomed. Mater. 34, 264–272. https://doi.org/10.1016/j.jmbbm.2014.02.013.

Moore, A.C., Burris, D.L., 2017. Tribological rehydration of cartilage and its potential role in preserving joint health. Osteoarthritis Cartilage 25, 99–107. https://doi.org/10.1016/j.joca.2016.09.018.

Moore, A.C., Burris, D.L., 2014. An analytical model to predict interstitial lubrication of cartilage in migrating contact areas. J. Biomech. 47, 148–153. https://doi.org/10.1016/j.jbiomech.2013.09.020.

Moshtagh, P.R., Korthagen, N.M., van Rijen, M.H.P., Castelein, R.M., Zadpoor, A.A., Weinans, H., 2018. Effects of non-enzymatic glycation on the micro- and nano-mechanics of articular cartilage. J. Mech. Behav. Biomed. Mater. 77, 551–556. https://doi.org/10.1016/j.jmbbm.2017.09.035.

Mow, V.C., Ratcliffe, A., Robin Poole, A., 1992. Cartilage and diarthrodial joints as paradigms for hierarchical materials and structures. Biomaterials 13, 67–97. https://doi.org/10.1016/0142-9612(92)90001-5.

Mow, V.C., Kuei, S.C., Lai, W.M., Armstrong, C.G., 1980. Biphasic creep and stress relaxation of articular cartilage in compression: theory and experiments. J. Biomech. Eng. 102, 73–84. https://doi.org/10.1115/1.3138202.

Nagel, T., Kelly, D.J., 2013. Altering the swelling pressures within in vitro engineered cartilage is predicted to modulate the configuration of the collagen network and hence improve tissue mechanical properties. J. Mech. Behav. Biomed. Mater. 22, 22–29. https://doi.org/10.1016/j.jmbbm.2013.03.017.

Nguyen, A.M., Levenston, M.E., 2012. Comparison of osmotic swelling influences on meniscal fibrocartilage and articular cartilage tissue mechanics in compression and shear. J. Orthop. Res. Off. Publ. Orthop. Res. Soc. 30, 95–102. https://doi.org/10.1002/jor.21493.

Nugent, G.E., Aneloski, N.M., Schmidt, T.A., Schumacher, B.L., Voegtline, M.S., Sah, R.L., 2006. Dynamic shear stimulation of bovine cartilage biosynthesis of proteoglycan 4. Arthritis Rheum. 54, 1888–1896. https://doi.org/10.1002/art.21831.

Oliver, W.C., Pharr, G.M., 2004. Measurement of hardness and elastic modulus by instrumented indentation: advances in understanding and refinements to methodology. J. Mater. Res. 19, 3–20. https://doi.org/10.1557/jmr.2004.19.1.3.

Oliver, W.C., Pharr, G.M., 1992. An improved technique for determining hardness and elastic modulus using load and displacement sensing indentation experiments. J. Mater. Res. 7, 1564–1583. https://doi.org/10.1557/JMR.1992.1564.

Oyen, M.L., 2013. Nanoindentation of biological and biomimetic materials. Exp. Tech. 37, 73–87. https://doi.org/10.1111/j.1747-1567.2011.00716.x.

Raviv, U., Klein, J., 2002. Fluidity of bound hydration layers. Science 297, 1540–1543. https://doi.org/10.1126/science.1074481.

Schätti, O.R., Gallo, L.M., Torzilli, P.A., 2016. A model to study articular cartilage mechanical and biological responses to sliding loads. Ann. Biomed. Eng. 44, 2577–2588. https://doi.org/10.1007/s10439-015-1543-9.

Schinagl, R.M., Ting, M.K., Price, J.H., Sah, R.L., 1996. Video microscopy to quantitate the inhomogeneous equilibrium strain within articular cartilage during confined compression. Ann. Biomed. Eng. 24, 500–512. https://doi.org/10.1007/BF02648112.

Shoaib, T., Yuh, C., Wimmer, M.A., Schmid, T.M., Espinosa-Marzal, R.M., 2020. Nanoscale insight into the degradation mechanisms of the cartilage articulating surface preceding OA. Biomater. Sci. 8, 3944–3955. https://doi.org/10.1039/D0BM00496K.

Silva, M., Shepherd, E.F., Jackson, W.O., Dorey, F.J., Schmalzried, T.P., 2002. Average patient walking activity approaches 2 million cycles per year: pedometers under-record walking activity. J. Arthroplasty 17, 693–697.

Spilker, R.L., Suh, J.-K., Mow, V.C., 1990. Effects of friction on the unconfined compressive response of articular cartilage: a finite element analysis. J. Biomech. Eng. 112, 138–146. https://doi.org/10.1115/1.2891164.

Swann, D.A., Slayter, H.S., Silver, F.H., 1981. The molecular structure of lubricating glycoprotein-I, thBeoundary lubricant for articular cartilage. JBC 256, 5921–5925.

Torzilli, P.A., 1985. Influence of cartilage conformation on its equilibrium water partition. J. Orthop. Res. 3, 473–483. https://doi.org/10.1002/jor.1100030410.

Treviño, R., Stoia, J.P., Laurent, M.A., Pacione, C., Chubinskaya, S., Wimmer, M.A., 2016. Establishing a live cartilage-on-cartilage interface for tribological testing. Biotribology 9. https://doi.org/10.1016/j.biotri.2016.11.002.

Trevino, R.L., Pacione, C.A., Malfait, A.-M., Chubinskaya, S., Wimmer, M.A., 2017. Development of a cartilage shear-damage model to investigate the impact of surface injury on chondrocytes and extracellular matrix wear. Cartilage 8, 444–455. https://doi.org/10.1177/1947603516681133.

Verzijl, N., DeGroot, J., Ben, Z.C., Brau-Benjamin, O., Maroudas, A., Bank, R.A., Mizrahi, J., Schalkwijk, C.G., Thorpe, S.R., Baynes, J.W., Bijlsma, J.W.J., Lafeber, F. P.J.G., TeKoppele, J.M., 2002. Crosslinking by advanced glycation end products increases the stiffness of the collagen network in human articular cartilage: a possible mechanism through which age is a risk factor for osteoarthritis. Arthritis Rheum. 46, 114–123. https://doi.org/10.1002/1529-0131(200201)46:1<114::AID-ART10025>3.0.CO;2-P.

Wahlquist, J., DelRio, F.W., Randolph, M., Aziz, A., Heveran, C., Bryant, S., Neu, C.P., Ferguson, V.L., 2017. Indentation mapping revealed poroelastic, but not viscoelastic, properties spanning native zonal articular cartilage. Acta Biomater. 64.

Waldstein, W., Perino, G., Gilbert, S.L., Maher, S.A., Windhager, R., Boettner, F., 2016. OARSI osteoarthritis cartilage histopathology assessment system: a biomechanical evaluation in the human knee. J. Orthop. Res. 34, 135–140. https://doi.org/10.1002/jor.23010.

Wang, C.C.-B., Hung, C.T., Mow, V.C., 2001. An analysis of the effects of depth-dependent aggregate modulus on articular cartilage stress-relaxation behavior in compression. J. Biomech. 34, 75–84. https://doi.org/10.1016/S0021-9290(00)00137-8.

Werthel, J.D., Schoch, B., Adams, J.E., Schleck, C., Cofield, R., Steinmann, S.P., 2018. Hemiarthroplasty is an option for patients older than 70 Years with glenohumeral osteoarthritis. Orthopedics 41, 222–228. https://doi.org/10.3928/01477447-20180621-03.

Wimmer, M.A., Pacione, C., Yuh, C., Chan, Y.-M., Kunze, J., Laurent, M.P., Chubinskaya, S., 2020. Articulation of an alumina-zirconia composite ceramic against living cartilage – an in vitro wear test. Journal of the Mechanical Behavior of Biomedical Materials 103, 103531. https://doi.org/10.1016/j.jmbbm.2019.103531.

Wimmer, M.A., Grad, S., Kaup, T., Hänni, M., Schneider, E., Gogolewski, S., Alini, M., 2004. Tribology approach to the engineering and study of articular cartilage. Tissue Eng. 10, 1436–1445. https://doi.org/10.1089/ten.2004.10.1436.

Zappone, B., Ruths, M., Greene, G.W., Jay, G.D., Israelachvili, J.N., 2007. Adsorption, lubrication, and wear of lubricin on model surfaces: polymer brush-like behavior of a glycoprotein. Biophys. J. 92, 1693–1708. https://doi.org/10.1529/biophysj.106.088799.